Manuscript

Urban Analytics and City Science

EPB: Urban Analytics and City Science
2022, Vol. 0(0) 1–15

DOI: 10.1177/23998083221083677
journals.sagepub.com/home/epb
SAGE

Temporal change in relationships between urban structure and surface temperature

Justin D Stewart
Department of Ecological Science, Vrije Universiteit Amsterdam, Amsterdam, The Netherlands; Department of Geography and the Environment, Villanova University, Radnor, PA, USA

Peleg Kremer
Department of Geography and the Environment, Villanova University, Radnor, PA, USA

Abstract

Surface temperature influences human health directly and alters the biodiversity and productivity of the environment. While previous research has identified that the composition of urban landscapes influences the physical properties of the environment such as surface temperature, a generalizable and flexible framework is needed that can be used to compare cities across time and space. This study employs the Structure of Urban Landscapes (STURLA) classification combined with remote sensing of New York City's land surface temperature (LST). These are then linked using machine learning and statistical modeling to identify how greenspace and the built environment influence urban surface temperature. Further, changes in urban structure are then connected to changes in LST over time. It was observed that areas with urban units composed of largely the built environment hosted the hottest temperatures while those with vegetation and water were coolest. Likewise, this is reinforced by borough-level spatial differences in both urban structure and heat. Comparison of these relationships over the period between 2008 and 2017 identified changes in surface temperature that are likely due to the changes in the presence of water, low-rise buildings, and pavement across the city. This research reinforces how human alteration of the environment changes LST and offers units of analysis that can be used for research and urban planning.

Keywords

Structure of urban landscapes, urban structure, surface temperature, spatial-temporal change, new york city

Corresponding author:
Peleg Kremer, Department of Geography & the Environment, Villanova University, 800 Lancaster Avenue, Villanova, PA 19085, USA.
Email: peleg.kremer@villanova.edu

Introduction

By 2030, it is projected that the majority of humanity will live in urban areas (DeSA, 2015), which are globally the fastest growing biome (Grimm et al., 2008). The analysis of the urban landscape and ecosystem services provided over time can be used to inform management practices to encourage urban resilience (McPhearson et al., 2014; Walker et al., 2004) under global change scenarios. It is critical to identify patterns and processes of urban structure-function relationships over time using a reproducible and scalable framework to meet and exceed the UN Sustainable Development Goals by 2030 (Lu et al., 2015). One of the key challenges that still persist in creating sustainable cities is that landscape topology is highly heterogeneous, and thus small spatial scale analyses are rapidly needed.

Quantifying land surface temperature (LST), a physical property of the environment, is of particular interest. In general, urban areas act as hotspots for elevated LST that are higher than surrounding rural areas (Streutker, 2003). However, much of the variation in LST also occurs within cities (Azhdari et al., 2018; Guo et al., 2020; Hamstead et al., 2016; Kremer et al., 2018). The spatial variation of LST within the urban landscape is measured at a point in time and thus will also change over time.

Numerous ecosystem aspects are subject to selective pressures of LST across functional (Morales et al., 2019) and taxonomic (Albright et al., 2011) scales of biodiversity (García et al., 2018; Jenerette et al., 2007). Social and economic variables are also correlated with urban heat, including race (Huang and Cadenasso, 2016; Sanchez and Reames, 2019), income (Huang and Cadenasso, 2016; Wong et al., 2016), and education (Wong et al., 2016). Understanding how LST is structured across the urban landscape can help enhance sustainability, such as reducing residential water use (Guhathakurta and Gober, 2007; Zhou et al., 2017), and even social inequalities. Likewise, landscape changes related to urbanization processes from vegetation to the built environment have been linked to urban LST (Oke, 1995; Zhou et al., 2011). Within the context of these covariates, remote sensing of LST is often used as a proxy for the spatial distribution of multiple ecological variables and human well-being.

Urban classification systems are used to identify important spatial and temporal processes such as LST in cities and overcome the challenge of urban heterogeneity. Local Climate Zones (LCZs) are offered in the literature as a method for identifying spatial and temporal patterns (Stewart and Oke, 2012; Yang et al., 2020). However, in many applications of the LCZ system, the three-dimensional aspect (building height) is inferred from the amount of sky visible instead of being directly measured as was done for many cities in Europe (Demuzere et al., 2019). Furthermore, LCZs also use a relatively coarse (30 m^2) resolution that may obstruct the impact of smaller or densely grouped infrastructures in cities on urban processes. Given building height has been shown to greatly influence urban processes such as albedo (Yang and Li, 2015) and LST (Chen et al., 2020), an explicit classification system that uses actual building heights at smaller spatial scales could be useful and compliment the commonly used LCZ system for more nuanced analyses.

STructure of URban LAndscape (STURLA) classification studies have demonstrated that urban structure can be explained by a discrete number of heterogeneously distributed three-dimensional 120 m^2 pixels composed of differing landscape elements (e.g., trees or high-rise buildings) (Hamstead et al., 2016). Previously, STURLA has been used to investigate LST (Hamstead et al., 2016; Kremer et al., 2018; Larondelle et al., 2014; Mitz et al., 2021), microbial diversity (Stewart et al., 2021), and air pollution (Cummings et al., 2022). STructure of URban LAndscape explicitly uses the height of buildings in cities from publicly available records and thus may be more meaningful for urban planners and designers when planning infrastructure. Likewise, STURLA has a relatively large number of potential classes (>200), and thus could potentially pick up patterns and processes that would otherwise be missed by smaller class sized systems such as LCZs (<20

classes). Land surface temperature variation is amplified and modified by vertical structures. For example, a high-rise building casting a shadow and thus cooling an adjacent parcel of land (Kremer et al., 2018) may be unaccounted for in classification systems that are not (1) compositional and (2) directly integrative of building height. As STURLA has both these attributes, it may offer a more flexible and dynamic framework that can take interactions between these landscape elements into account. Such interactions, which may influence ecological and environmental parameters, such as LST, are unaccounted for in other models where individual pixels represent a single quantity such as pavement or grass.

STructure of URban LAndscape offers a simple way to understand units of urban structure that can be applied to planning efforts for sustainable development across cities and over years. The goal of this study is to demonstrate that STURLA is a useful alternative and an additional classification system to understand urban processes over time. In this paper, we apply STURLA to a spatial-temporal process for the first time and link changes in urban structure to changes in LST in New York City (NYC) through remote sensing and machine learning.

Material and methods

Site description

New York City is the largest city in the United States of America with a 2019 estimated population of over an estimated 8,336,800 residents (United States Census Burough, 2016) covering an area of ~740 km^2. Located in the eastern part of the continental United States, NYC is split into five boroughs (Brooklyn, The Bronx, Queens, Staten Island, and Manhattan) of varying size, populations, and socio-economic class.

Urban structure

The STURLA classification for NYC for the years 2008 and 2017 was constructed following previous studies (Cummings et al., 2022; Hamstead et al., 2016; Mitz et al., 2021) by joining land cover raster data (United States Geological Survey (USGS) National land cover database 3.0 foot resolution) and parcel level building height data. Building height was accessed from the NYC MapPluto database (NYC Department of City Planning, 2021) for each year. A fishnet grid with 120 m^2 pixels was overlaid on the combined land cover and building height dataset. STructure of URban LAndscape classifications for each cell were determined based on the presence of each urban structure component identified. Each letter in the STURLA code represents a different component of the urban environment. Each classification of a STURLA cell indicates a specific combination of different urban structure components: trees (t), grass (g), bare soil (b), water (w), pavement (p), low-rise buildings (1–3 stories) (l), mid-rise buildings (4–9 stories) (m), and/or high-rise buildings (9+ stories) (h). For example, if any percentage greater than 0.0% of trees, grass, pavement, and low-rise buildings is present, that pixel will be coded with *tgpl*. Using the zonal statistics tabulate area operation, we computed the area of a combined land cover and building height dataset within each cell. Examples of coded STURLA pixels can be found in Figure 1(a) and Table 1. Maps of example parks (Supplementary Figure 1) and boroughs (Supplementary Figure 2) can be found in the supplementary materials for reference.

Land surface temperature acquisition and processing

Land surface temperature data were accessed from the USGS Earth Explorer using Landsat 7 Analysis Ready Data (ARD). Analysis Ready Data are corrected, pre-processed, and converted to

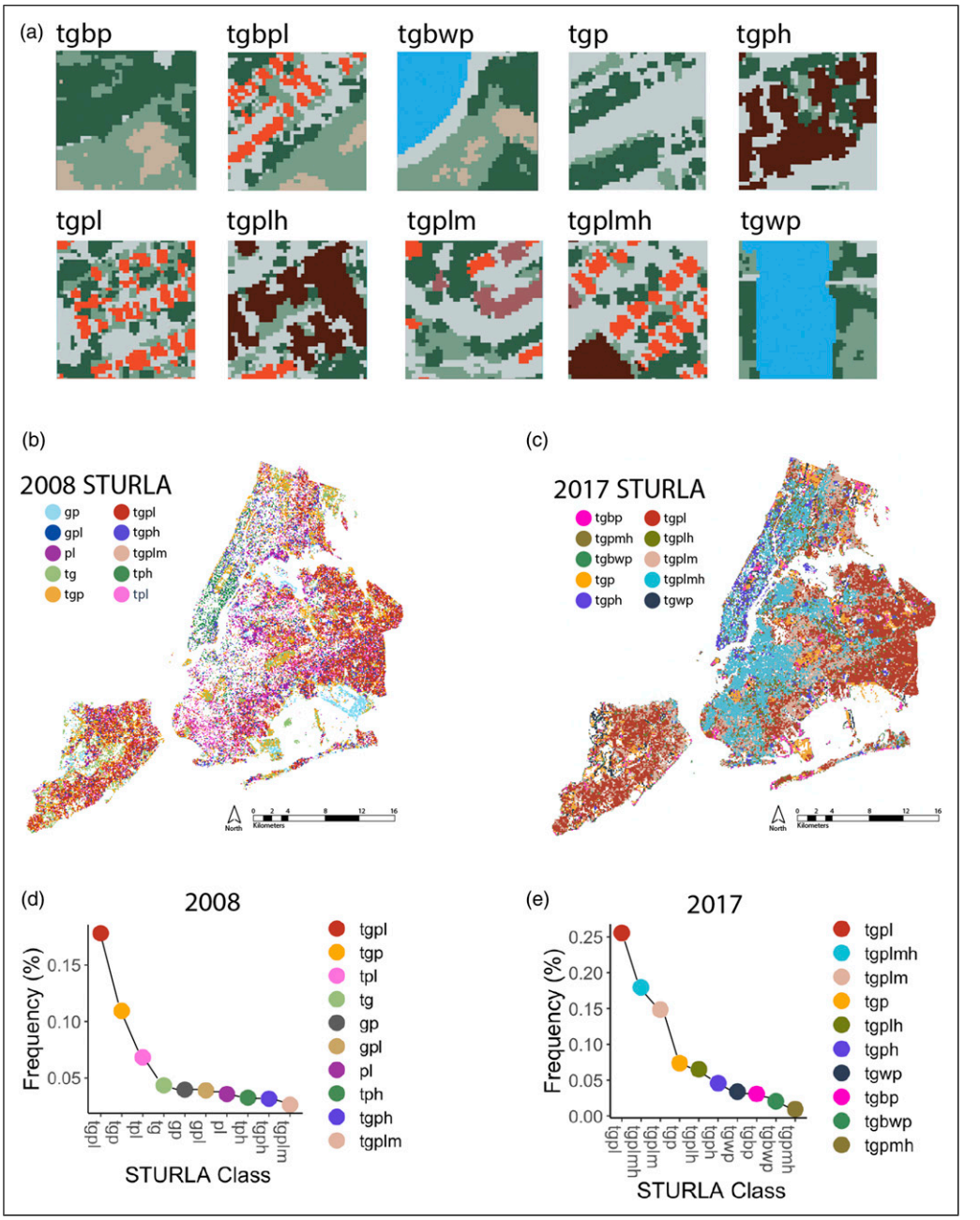

Figure 1. (a). Examples of the most frequent STURLA classes in NYC 2008 colored by landscape component (trees: dark green, grass: light green, bare soil: beige, pavement: gray, bright red: low-rise buildings, medium red: mid-rise buildings, and dark red: high-rise buildings). (b). Map of the spatial distribution of STURLA classes for NYC 2008. (c). Map of the spatial distribution of STURLA classes for NYC 2017. (d). Ranked frequency plot of STURLA classes in NYC 2008. (e). Ranked frequency plot of STURLA classes in NYC 2017. Note: STURLA: structure of urban landscapes; NYC: New York City.

Table 1. STURLA landscape element magnitude and direction estimation. This table contains the correlation coefficients (Rho) from permutational Spearman correlations. Bold values indicate $p < 0.05$ for the correlation model. All other correlations were insignificant.

Landscape element	LST 2008 Rho	LST 2017 Rho	Δ LST Rho
Trees (t)	−**0.30**	−**0.38**	−0.07
Grass (g)	−0.23	−**0.52**	−0.05
Bare soil (b)	−0.12	−**0.30**	−**0.22**
Water (w)	−0.09	−**0.55**	−**0.25**
Paved (p)	**0.34**	**0.65**	−0.07
Low-rise (l)	0.19	**0.52**	**0.38**
Mid-rise (m)	0.33	**0.33**	**0.21**
High-rise (h)	−0.13	**0.31**	0.03

Note: STURLA: STructure of Urban LAndscapes; LST: land surface temperature.

LST (in degrees Celsius) by the USGS. It is worth noting that some Landsat striping is present in the data that may influence the results. All LST values are representative of areas where the satellite could sample such as building roofs or pavement and not air temperature. It is worth nothing that LST is being measured and not temperatures inside buildings or their walls, which are meaningful for heat-human health studies; however, remotely sensed LST is a commonly used proxy and may be meaningful for other ecosystem processes. After downloading, the mean zonal statistics were calculated per STURLA pixel for each raster. All available LST rasters for the defined time period that contained less than 30% cloud cover over the NYC boundaries were used. The time period was chosen as between June 21st and September 22nd for each year as it would allow us to look at both the mean across days and the variance between them (Hamstead et al., 2016; Mitz et al., 2021). These provide a wide representation of summer temperatures to validate that STURLA identifies patterns between urban structure and LST and thus can be used in future urban planning practices. All remote sensing images were taken during the daytime with similar solar geometries. Temperature anomalies were found on 07/22/08 and 08/24/17 (see Figure 2(c) and (d)) and were left in the analyses as they may represent a normal variation in summer temperatures rather than an instrument error. To validate that LST trends observed between the 2 years were not heavily subject to climatic/weather anomalies, a permutation Pearson correlation model was constructed (see Supplementary Figure 3). A high degree of correlation between the years suggests that the years have similar heat signatures, where a larger deviance would suggest the presence of an anomaly. This model revealed significant and strong relationships between the 2 years and suggests that direct comparisons of the 2 years are acceptable; however, it does not fully remove the possibility that an anomaly may be present.

Data analysis and visualization

All datasets were projected to NAD 1983 State Plane New York Long Island FIPS 3104 Meters. Quantile classification (5 groups) is used in all maps for visualization as this allows for comparison of the distribution of data across the years. It is worth noting that other visualization methods such as natural breaks may produce different visualizations but do not influence the statistical results. Statistical analysis was done in R. 4.0.1. The similarity of LST hosted in STURLA classes was determined using hierarchical clustering with Bray-Curtis dissimilarity. This method was chosen as it is qualitative and allows for compositional comparison between LST by STURLA class (Figure 2(c) and (d)). Land surface temperature values were visualized with a heatmap using scaled and

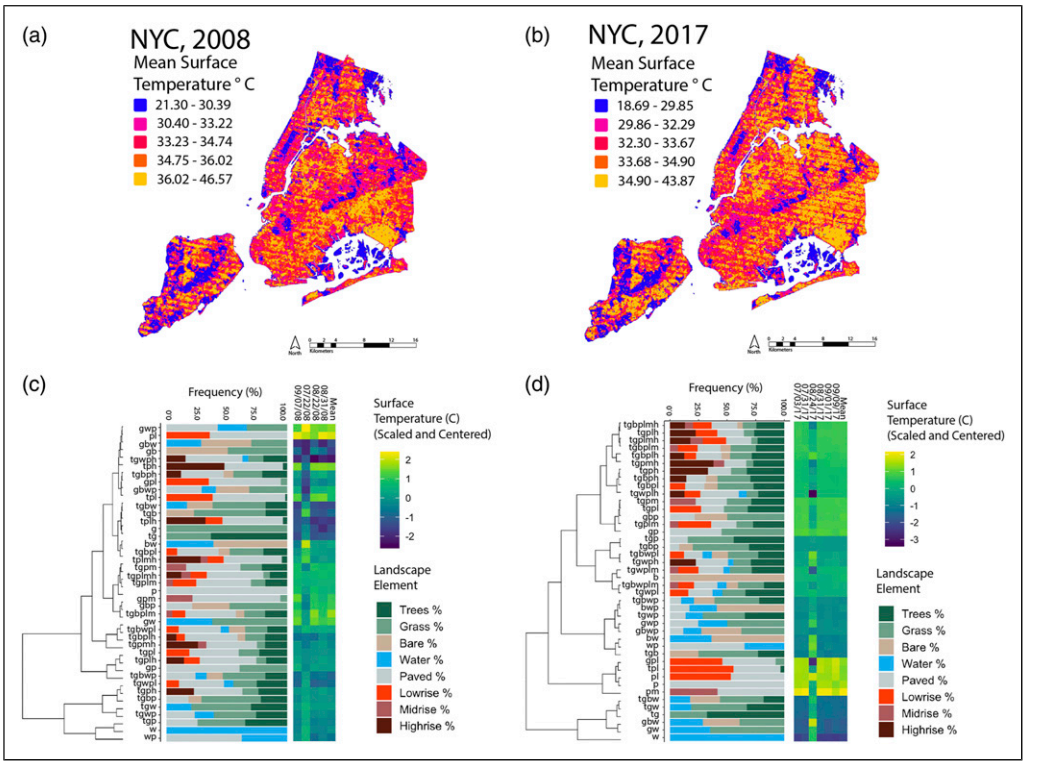

Figure 2. ((a): 2008, (b): 2017) Map of LST in NYC where colors closer to blue indicate lower values and closer to red being higher. ((c): 2008, (d): 2017) Hierarchically clustered heatmap of LST values showing the LST for each day the mean value as the final column on the right. Between the heatmap and the dendrogram, a stacked barplot of the mean internal landscape compositions for each STURLA class is shown. The reader is encouraged to download and zoom into this figure if interested in specific STURLA classes. Note: STURLA: Structure of Urban Landscapes; LST: land surface temperature; NYC: New York City.

centered data to allow comparability between the years. Landscape heterogeneity (# internal landscape elements per pixel) was calculated as the sum of landscape elements within a pixel (comprising 1 STURLA class) for all years, and change was calculated as the heterogeneity in a pixel of 2008 minus that of 2017. For example, STURLA class *bpl* has a heterogeneity value of 3. This calculation could miss changes in classes that have retained the same number of landscape elements, such as a transition from tpg to bpw and is worth noting. Change in surface temperature likewise was calculated as 2008 LST minus 2017 LST.

Supervised machine learning, random forest regression, models using the *caret* package (Kuhn, 2008) were used to estimate the strength of the relationship between STURLA classes and mean LST per class. This model was chosen because it was previously shown to better handle non-parametric spatial data when compared to linear models (Chen et al., 2017; Oliveira et al., 2012). Classes with less than 100 pixels were removed as these more infrequent classes likely have less of a role in overall patterns of surface temperature. Models were built as: Mean LST per STURLA class ~ Trees % + Grass % + Bare Soil % + Water % + Pavement % + Low-rise % + Mid-rise % + High-rise %. For this, the data were partitioned into 60% training and 40% validation sets that underwent 10-fold repeated cross validation. Trained models were then used to predict mean LST when given a STURLA class, which were then projected to each pixel in the STURLA grid. The root mean

squared error (RMSE) was used to quantify average model error. Variable importance was measured using the *varImp* function and then scaled from 0 to 100 where values closer to 100 are more important for model accuracy and error reduction. The same process was applied to identify the mean change in LST per STURLA class and the mean change in landscape component percentages. To better represent model results, the top and bottom 1.0% of model predictions and subsequent errors were excluded from mapping.

To account for spatial and temporal autocorrelation, permutational methods were used to estimate a distribution from which to generate a *p*-value. This means that the distribution is not structured through a spatial process, as the randomization breaks this down by resampling the parameter values. It is worth noting that even with models that destroy autocorrelative structure, some autocorrelation may be present. Permutational Spearman correlations using *wPerm* (Weiss, n.d.) were used to identify relationships between individual STURLA landscape elements (e.g., *h*) with LST for each year as well as change in LST. Permutation also allows for comparison of LST as the values for each year are drawn from a similar urban landscape and thus a similar underlying distribution. Differences in changes in STURLA heterogeneity and LST by borough were tested using permutational T-tests using the package *RVAideMemoire* (Hervé, 2020). Data and code for these analyses can be found at: https://github.com/thecrobe/STURLA_NYCChange.

Results

New York City STURLA structure

The 10 most frequent STURLA classes (Figure 1(a)) explained 60.84% and 80.01% of NYC's structure in 2008 and 2017, respectively (Figure 1(d) and (e)). For 2008 and 2017, only 15 STURLA classes contained exclusively the natural environment (classes composed of combinations of *t, g, b,* and *w*) that cover a mean between the years of 5.69% of NYC's landscape. In 2008, the most common STURLA class per borough was *tgpl* in Brooklyn (9.85%), Staten Island (26.32%), and Queens (24.36%). Class *tgp* dominated The Bronx (13.04%) and *tph* in Manhattan (19.94%).

In 2017, class *tgpl* was still the most frequent (and became more abundant) in Staten Island (36.46%) and Queens (34.37%). Relatively large changes in urban structure occurred in Brooklyn, The Bronx, and Manhattan. Class *tgplmh* dominated Brooklyn (34.79%) and demonstrated gains and transitions from the 2008 most abundant class, *tgpl*. Class *tgph* (21.58%) replaces *tph* as the most common in Manhattan. The Bronx grew vertically with class *tgplmh* becoming the most frequent (20.51%). The spatial distribution of STURLA classes was heterogenous; however, specific classes are clustered throughout the city (e.g., *tgp* in Highland Park and Floyd Bennet Field in Brooklyn). Likewise, classes with *h* were largely found in Manhattan (*tgph*) and Brooklyn (*tgplmh)*.

New York City surface temperature

New York City 2008 LST ranged from 21.30°C to 46.57°C across the urban landscape with a mean of 32.24°C. Each borough hosted unique LST values that significantly differed from each other (all $p < 0.002$) with the exception of The Bronx and Staten Island ($p = 0.48$) and Staten Island with Queens ($p = 0.992$). The hottest borough on average was Queens (34.19°C) followed by Brooklyn (33.83°C), The Bronx (32.62°C), Staten Island (32.59°C), and Manhattan (32.23°C). In 2017, NYC had a narrower range in LST compared to 2008 with from 18.23°C to 43.87°C with a higher mean of 32.77°C. For 2017 the hottest borough on average was still Queens (33.46°C) followed by Brooklyn (32.75°C), The Bronx (32.51°C), Manhattan (32.19°C), and Staten Island (31.97°C). Similar to 2008, in 2017 each borough hosted unique LST values that significantly differed ($p < 0.002$) from

each other still excluding The Bronx and Staten Island ($p = 0.48$). In contrast, Manhattan and Staten Island differed ($p = 0.778$) in LST signatures in 2008. While the LST signatures of each year's summer were highly correlated (R^2, slope = 0.9, Supplementary Figure 3), a slope of less than 1.0 may also suggest subtle changes in climate between the years; however, this is difficult to separate from the change in urban structure.

Distinct patterns of LST within the city were consistent across the years. Greenspaces such as Central Park in Manhattan hosted lower surface temperatures than the surrounding STURLA classes that have greater proportions of the built environment (Figures 1(b) and (c) and 2(a) and (b)). Similar patterns can be found in other parks/greenspaces across the city (e.g., Pelham Bay Park, Staten Island Greenbelt, and Prospect Park in Brooklyn). Land surface temperature was highest in STURLA classes where the built environment dominated (Figure 2(c) and (d), e.g., *gpl, tpl, p, pl,* and *pm*). Likewise, LST was lowest in STURLA classes where there was no built environment (Figure 2(c) and (d), e.g., *tgbw, tgw, gbw, gw,* and *w*). These patterns are intensified in 2017 as the built environment (classes with *p, l, m,* and *h*) clusters more than in 2008 and host the highest LST across the landscape. Conversely, STURLA classes with water cluster more readily and host the lowest LST.

Change in urban structure and surface temperature

New York City's urban structure became more homogenous as the number of STURLA classes decreased from 139 classes in 2008 to 118 classes in 2017; however, individual STURLA pixels generally became more heterogenous and gained landscape elements (Figure 3(b), e.g., *t* or *p*). Water was the least common feature, and STURLA classes with water did not change greatly, with the exception of areas largely located in Staten Island and Jamaica Bay. Changes in STURLA classes were not uniform as some STURLA pixels changed greatly, for example, the addition of a green roof in Figure 3(a), while others remained relatively the same. An average of +1.344 landscape elements were gained (Figure 3(b), e.g., a tpl pixel in 2008 gaining *g* and becoming *tgpl*). On average, Manhattan (+1.768) gained the most internal landscape elements, followed by Brooklyn (+1.626), The Bronx (+1.544), Queens (+1.123), and Staten Island (+1.097). Each borough gained STURLA class elements differently (all $p < 0.002$). STructure of URban LAndscape classes composed of a mixture of the built and natural environment (e.g., Midtown Manhattan and Brooklyn) experienced greater gains in the number of STURLA elements across the city as compared to greenspaces (e.g., parks) which became more homogenous despite additions of different landscape elements.

Across NYC as a whole, LST per pixel increased from 2008 to 2017 by a mean of +0.47°C (Figure 3(c)). Changes in LST also varied by borough ($p > 0.002$), with the exception of The Bronx with Manhattan ($p = 0.454$), Manhattan with Queens ($p = 0.084$), and Queens with Staten Island ($p = 0.966$). Decreases in LST were largely found in Brooklyn, South Queens, Central Staten Island, and the South Bronx. LST increased in North Queens, Manhattan, and South Staten Island. Land surface temperature change for the 10 most frequent classes were *tgpl* (−3.57°C), *tgplmh* (−2.88°C), *tgplm* (−3.49°C), *tgp* (+0.212°C), *tgplh* (−3.30°C), *tgph* (−2.29°C), *tgwp* (+1.24°C), *tgbp* (+0.24°C), *tgbwp* (+0.92°C), and *tgpmh* (−2.76°C).

The change in LST modeled as a function of changes in internal STURLA components (e.g., mean percentage of *t* decreasing 0.03% in class *tgpl*) revealed a moderate relationship (Figure 3(e), $R^2 = 0.433$, RMSE: 2.72°C). This association was driven by changes in water (Supplementary Figure 5), low-rise buildings, and pavement (all variable importance >25%). Likewise, modeling at the STURLA class level outperforms correlations between individual STURLA elements (e.g., change in LST ~ change in percentage *t*) (Table 1). Univariate correlations between change in LST demonstrated significant ($p > 0.05$) relationships with bare soil, water, low-rise, and mid-rise within

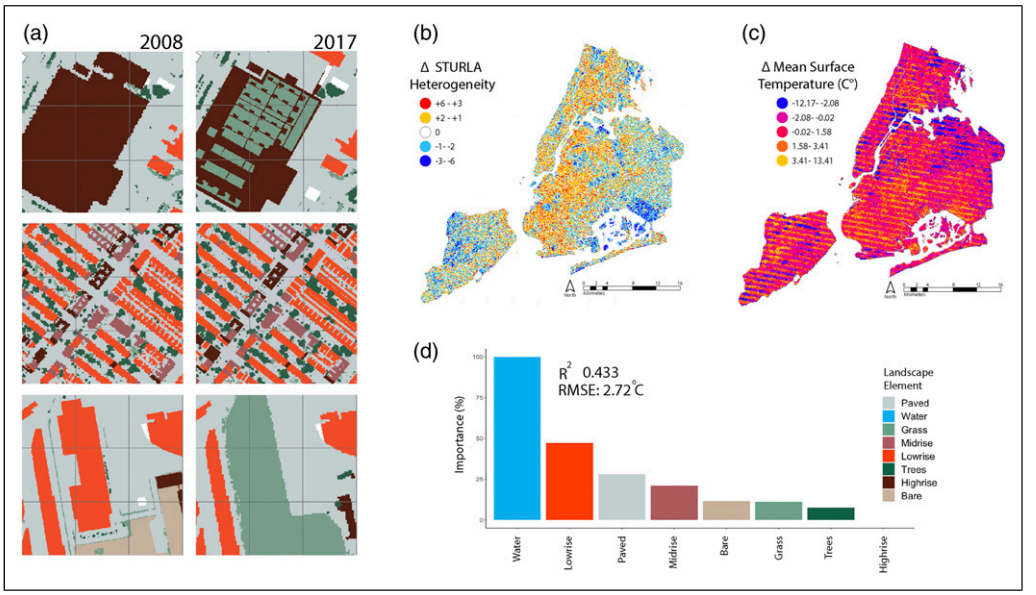

Figure 3. (a). Example of STURLA pixels that underwent different degrees of change in structure. (b). Map of change in STURLA class heterogeneity. (c). Map of change in mean surface temperature. (d). Random forest regression variable importance for Δ LST as a function of Δ in landscape element percentages. Note: STURLA: Structure of Urban Landscapes; LST: land surface temperature.

STURLA class percentages (Table 1). Land surface temperature decreased with increasing amounts of bare soil and water while the opposite relationships were observed for the built environment. A permutational model testing the relationship between LST in 2008 to LST in 2017 per STURLA pixel revealed a strong positive correlation (Supplementary Figure 1, R^2: 0.815, $p < 0.0001$) and suggests that the majority of variation in LST is due to urban structure; however, climatic trends may also influence this study's results but to a relatively small degree. Likewise, moderate to strong significant positive correlations were found between LST for each year when separated by STURLA class; however, the strength of the relationship varied by class (Supplementary Figure 4).

Land surface temperature prediction by STURLA class

STructure of URban LAndscape classes were able to explain and predict LST across NYC for both 2008 (R^2:0.788, RMSE:0.34°C) and 2017 (R^2:0.788, RMSE: 1.90°C) better than any individual within class landscape element (Table 1). Despite strong correlations between urban structure and LST, the relative role of STURLA internal class elements differed. 2008 models relied on paved, trees, high-rise, grass, and bare soil to predict LST (Figure 4(a), all variable importance >25%). In contrast, 2017 LST was largely predicted by the presence and distribution of STURLA classes with pavement and water (Figure 4(d), all variable importance >25%). Both models predicted higher LST in classes hosting the built environment (e.g., *tgplm*, Figures 4(b) and (e)) and lower temperatures in those that are partially vegetated (e.g., *tgp* and *tg*). Predicted values were greater in 2017 than 2008. Models overpredicted LST in areas with greenspace (e.g., parks) and STURLA classes dominated by bare soil for both years (Figures 4(c) and (f)). In contrast, they underpredicted where classes *tgpl* and *tgplmh* dominated.

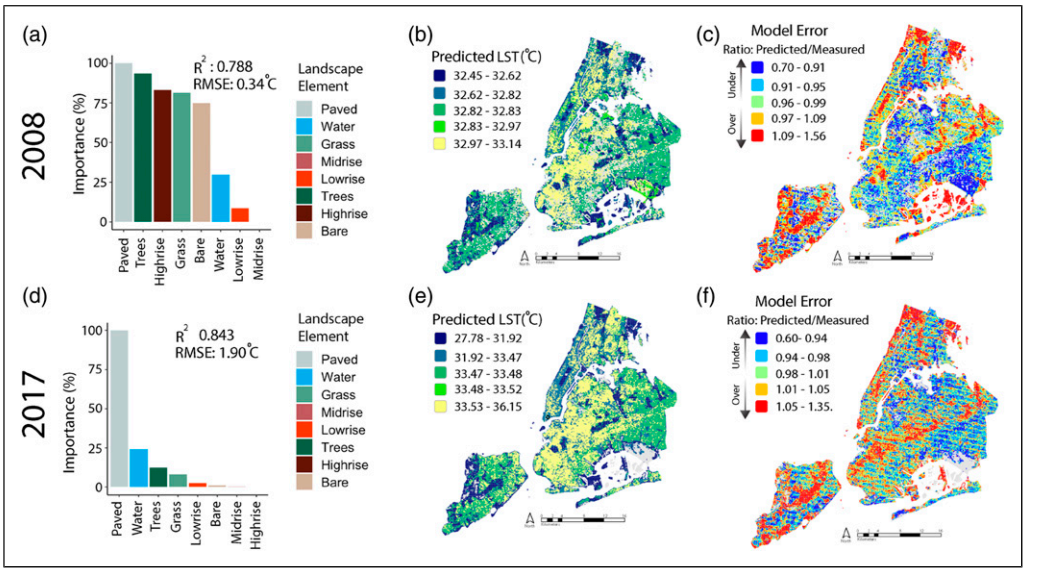

Figure 4. ((a): 2008, (d): 2017) Random forest regression variable importance for LST prediction with coefficient and error at the top left. ((b): 2008, (e): 2017) Map of predicted LST per STURLA class where darker colors indicate lower LST and lighter colors being higher LST. ((c): 2008, (f): 2017) Model error from random forest regression shown as a ratio of predicted/measured LST. Note: STURLA: Structure of Urban Landscapes; LST: land surface temperature.

Univariate correlations estimate the direction of each variable on STURLA class LST as it cannot be inferred from random forests. In 2008, percentage paved had significant positive relationships with LST. For 2017, all within class elements had significant relationships ($p > 0.05$) with LST. As percentages of trees, grass, bare soil, and water increase, mean LST per STURLA class decreased. The opposite relationship was found where LST increased as the percentages of the built environment (paved, low-rise, mid-rise, and high-rise) also increased.

Discussion

New York City urban structure

The urban landscape for both years was unsurprisingly dominated by STURLA classes in the built environment with the exception of established parks and greenspaces. The top 10 classes found in each year varied greatly with both transitions from the most prevalent STURLA classes to new urban forms as well as differences in their distribution. 2017 became more homogenous as demonstrated by the top 10 classes explaining a greater proportion of NYC's landscape as compared to 2008. However, the small spatial scale nature of STURLA allowed for identification of change in urban heterogeneity, that is, the reduction of 21 classes, which may be overlooked with classification systems at larger spatial scales. Likewise, the city as a whole grew vertically as *l*, *m*, and *h* STURLA elements were commonly added. Brooklyn experienced the greatest change in the vertical dimension as classes *tgpl* and *tgp* transitioned to *tgplmh*. With the growth in these vertical landscape elements, a relative shift in the internal landscape proportions of the classes in Brooklyn and The Bronx occurs as a function of STURLA's compositional (elements sum to 1) nature.

3D urban structure influences surface temperature over time

STructure of URban LAndscape captured the urban structure-heat relationship as demonstrated by STURLA classes hosting unique LST values and robust correlations with relatively low error across the urban landscape across time and space. Changes in urban structure were able to partially explain changes in LST across the years. Variation in LST was largely attributed to compositional changes in the proportions of water and the built environment (low-rise, mid-rise buildings, and pavement). This is logical given the large heat capacity of water; thus, a small amount would have a considerable influence on a STURLA pixel's heat signature as was seen with the water added largely in Staten Island and Jamaica Bay. Likewise, low-rise and mid-rise buildings are prevalent in NYC and are cheaper to build/demolish in a short period of time. This contrasts with the addition/removal of high-rise buildings, which logistically should take longer and be less frequent. These results further support that urban heat can be influenced by building height and shape (Palme et al., 2018; Stewart and Oke, 2012).

Furthermore, STURLA models displayed better associations and more robust predictions than other 2-dimensional models of urban structure (Connors et al., 2013). This is due to each STURLA class being able to contain differing percentages of each landscape element, thus offering a more realistic representation of urban structure. Despite this, limitations do exist, for example, two pixels of STURLA class *gwp* may contain vastly differing percentages of grass, water, and pavement. These compositional variations may be sources of error in models as a function of uncertainty propagation. Likewise, the within class variation and neighborhood effects of nearby pixels of same or different STURLA classes may be influencing local LST signatures as demonstrated in Berlin (Kremer et al., 2018). This could be seen where a pixel coded as STURLA class *p* neighbors a *tgph* pixel that may cast a shadow on the *p* pixel and thus cool the first pixel's relative LST compared to other *p* pixels across the city. It is worth noting that neighborhood effects would be present in other urban classification-function studies as well.

Our findings that STURLA classes composed largely of the built environment host higher LST values in both years complement studies in cities of varying sizes across the globe with different climates and biomes: Beijing (Kuang et al., 2015), Berlin (Kottmeier et al., 2007; Kremer et al., 2018), Lagos (OS and AA, 2016), Kunming (Chen and Zhang, 2017), Melbourne (Jamei et al., 2019), NYC (Hamstead et al., 2016; Susca et al., 2011), Phoenix (Buyantuyev and Wu, 2010; Connors et al., 2013), Tehran (Bokaie et al., 2016), and Vancouver (Voogt and Oke, 1998). Unsurprisingly, pixels and STURLA classes with greater proportions of greenspace (containing *t* and or *g*) hosted lower LST signatures. What is interesting here is that it further supports the notion that urban management can benefit from thinking of urban structure compositionally, as the greenspace in these classes likely confers lower heat signatures to the other landscape components (e.g., *p*).

STructure of URban LAndscape as an alternative and complementary to identifying urban heat patterns

STructure of URban LAndscape provides a way of understanding changes in urban heat as an addition to other popular methods such as LCZs. In fact, in this study, the STURLA model displayed higher correlations with LST over time than a study that employed LCZs in Hamburg, Germany (Bechtel, 2011). This supports the idea that the benefits of small spatial scale and explicit vertical height are important for urban structure modeling.

STructure of URban LAndscape allows the urban structure of a city to define the classification without a-priori binning of infrastructures into classes. With 255 potential combinations of urban structure that may or may not all be present in a city, it allows for high flexibility in explanatory power. This fidelity may complement the more generalized LCZ system that offers a smaller number

of classes, that is, 17, to describe urban structure. In most cities tested, STURLA only needs 15–25 classes to explain urban structure (Cummings et al., 2022; Hamstead et al., 2016; Mitz et al., 2021; Stewart et al., 2021), and thus, it is quite similar to LCZs but still provides room for novel urban structures to emerge and be classified. However, future studies of STURLA are needed to determine if these relationships are seen in other cities with differing climates and histories.

Another point of distinction in the STURLA method is that it incorporates the 3D shape of cities by using measured building height instead of estimating this from variables such as percentage sky view available (Demuzere et al., 2019). Lastly, STURLA works at small spatial scales that are meaningful for urban planners (120 m^2) as opposed to the 100s–1000s of meter scale of LCZs. While it has been well established that LST is largely dependent on building height, pavement, and greenspace (Stewart et al., 2014) (as is also demonstrated in this study), STURLA pixels are geographically meaningful for neighborhood development projects. Urban planners could evaluate different configurations and proportions of the built and natural environment using STURLA-based prediction and error models to best identify how to mitigate high LST in neighborhoods.

These properties of STURLA could be leveraged statistically as well to explain more nuanced microclimates by allowing the city itself to define its classification system. Likewise, STURLA classes could be updated in patches (per pixel or groups of pixels) that have changed urban form, such as a building being constructed, as this information becomes available, instead of relying on remotely sensed information that could be generated less frequently and subject to local weather conditions such as clouds. Further, STURLA provides meaningful and simple units of urban structure that could identify trends in urban processes, such as this study demonstrates with surface temperature, that could be applied to any city globally.

Conclusion

In this paper, we used remote sensing of urban heat with the STURLA method, which was linked together by machine learning and statistical modeling, to identify the urban spatial-temporal structure-surface temperature relationship in NYC over a decade. Understanding these dynamics is crucial to future sustainable and egalitarian urban planning, given how urban surface temperature influences human well-being and urban biodiversity. We conclude that NYC as a whole is becoming more homogenous by growing taller, largely in Brooklyn and Manhattan, and, on average, showed higher LST in 2018 compared to 2008. Likewise, these changes are linked to specific three-dimensional urban units where change in heat signatures is the prevalence and distribution of water, low-rise, and paved buildings. This study reinforces that STURLA is a computationally inexpensive model and aids in understanding LST effects and offers context for sustainable development and urban planning at small spatial scales. Limitations of this study include an analysis of only two timepoints, that STURLA is agnostic to the physical composition of building materials, and the influence of species and functional traits in the vegetative elements of a STURLA class. Future studies should incorporate other measures of urban ecosystems such as plant biodiversity.

Author contributions

Conceptualization: PK and JDS.
Formal data analysis: JDS and PK.
Writing: JDS and PK.

Declaration of conflicting interests

The author(s) declared no potential conflicts of interest with respect to the research, authorship, and/or publication of this article.

Funding

The author(s) disclosed receipt of the following financial support for the research, authorship, and/or publication of this article: This project is funded by NSF award # 1832407.

ORCID iDs

Justin D Stewart https://orcid.org/0000-0002-7812-5095
Peleg Kremer https://orcid.org/0000-0001-6844-5557

Supplemental material

Supplemental material for this article is available online.

References

Albright TP, Pidgeon AM, Rittenhouse CD, et al. (2011) Heat waves measured with MODIS land surface temperature data predict changes in avian community structure. *Remote Sensing of Environment* 115: 245–254. DOI: 10.1016/j.rse.2010.08.024.

Azhdari A, Soltani A and Alidadi M (2018) Urban morphology and landscape structure effect on land surface temperature: Evidence from Shiraz, a semi-arid city. *Sustainable Cities and Society* 41: 853–864. DOI: 10.1016/j.scs.2018.06.034.

Bechtel B (2011) Multitemporal Landsat data for urban heat island assessment and classification of local climate zones. In: 2011 Joint Urban Remote Sensing Event, JURSE 2011 - Proceedings, Munich, Germany, 11–13 April 2011, pp. 129–132. DOI: 10.1109/JURSE.2011.5764736.

Bokaie M, Zarkesh MK, Arasteh PD, et al. (2016) Assessment of Urban Heat Island based on the relationship between land surface temperature and Land Use/Land Cover in Tehran. *Sustainable Cities and Society* 23: 94–104. DOI: 10.1016/j.scs.2016.03.009.

Buyantuyev A and Wu J (2010) Urban heat islands and landscape heterogeneity: Linking spatiotemporal variations in surface temperatures to land-cover and socioeconomic patterns. *Landscape Ecology* 25: 17–33. DOI: 10.1007/s10980-009-9402-4.

Chen W, Xie X, Wang J, et al. (2017) A comparative study of logistic model tree, random forest, and classification and regression tree models for spatial prediction of landslide susceptibility. *Catena* 151: 147–160. DOI: 10.1016/j.catena.2016.11.032.

Chen X and Zhang Y (2017) Impacts of urban surface characteristics on spatiotemporal pattern of land surface temperature in Kunming of China. *Sustainable Cities and Society* 32: 87–99. DOI: 10.1016/j.scs.2017.03.013.

Chen Y, Wu J, Yu K, et al. (2020) Evaluating the impact of the building density and height on the block surface temperature. *Building and Environment* 168: 106493. DOI: 10.1016/J.BUILDENV.2019.106493.

Connors JP, Galletti CS and Chow WTL (2013) Landscape configuration and urban heat island effects: assessing the relationship between landscape characteristics and land surface temperature in Phoenix, Arizona. *Landscape Ecology* 28: 271–283. DOI: 10.1007/s10980-012-9833-1.

Cummings L. E., Stewart J. D., Kremer P. and Shakya K. M. (2022) Predicting citywide distribution of air pollution using mobile monitoring and three-dimensional urban structure. *Sustainable Cities and Society* 76: 103510.

Demuzere M, Bechtel B, Middel A, et al. (2019) Mapping Europe into local climate zones. *Plos One* 14(4): e0214474. DOI: 10.1371/JOURNAL.PONE.0214474.

DeSA U (2015) *World Population Projected to Reach 9.7 Billion by 2050*. New York, NY, USA: UN DESA United Nations Department of Economic and Social Affairs.

García FC, Bestion E, Warfield R, et al. (2018) Changes in temperature alter the relationship between biodiversity and ecosystem functioning. *Proceedings of the National Academy of Sciences of the United States of America* 115: 10989–10994. DOI: 10.1073/pnas.1805518115.

Grimm NB, Faeth SH, Golubiewski NE, et al. (2008) Global change and the ecology of cities. *Science* 319(5864): 756–760. DOI: 10.1126/science.1150195.

Guhathakurta S and Gober P (2007) The impact of the Phoenix urban heat Island on residential water use. *Journal of the American Planning Association* 73: 317–329. DOI: 10.1080/01944360708977980.

Guo A, Yang J, Sun W, et al. (2020) Impact of urban morphology and landscape characteristics on spatio-temporal heterogeneity of land surface temperature. *Sustainable Cities and Society* 63: 102443. DOI: 10.1016/j.scs.2020.102443.

Hamstead ZA, Kremer P, Larondelle N, et al. (2016) Classification of the heterogeneous structure of urban landscapes (STURLA) as an indicator of landscape function applied to surface temperature in New York City. *Ecological Indicators* 70: 574–585. DOI: 10.1016/j.ecolind.2015.10.014.

Hervé M (2020) *Package 'RVAideMemoire'*.

Huang G and Cadenasso ML (2016) People, landscape, and urban heat island: dynamics among neighborhood social conditions, land cover and surface temperatures. *Landscape Ecology* 31: 2507–2515. DOI: 10.1007/s10980-016-0437-z.

Jamei Y, Rajagopalan P, Sun Q, et al. (2019) Spatial structure of surface urban heat island and its relationship with vegetation and built-up areas in Melbourne, Australia. *Science of the Total Environment* 659: 1335–1351. DOI: 10.1016/j.scitotenv.2018.12.308.

Jenerette GD, Harlan SL, Brazel A, et al. (2007) Regional relationships between surface temperature, vegetation, and human settlement in a rapidly urbanizing ecosystem. *Landscape Ecology* 22: 353–365. DOI: 10.1007/s10980-006-9032-z.

Kottmeier C, Biegert C and Corsmeier U (2007) Effects of urban land use on surface temperature in berlin: case study. *Journal of Urban Planning and Development* 133(2): 128–137.

Kremer P, Larondelle N, Zhang Y, et al. (2018) Within-class and neighborhood effects on the relationship between composite urban classes and surface temperature. *Sustainability* 10(3): 645. DOI: 10.3390/su10030645.

Kuang W., Liu Y., Dou Y., Chi W., Chen G., Gao C. and Zhang R. (2015) What are hot and what are not in an urban landscape: quantifying and explaining the land surface temperature pattern in Beijing, China. *Landscape ecology* 30(2): 357–373.

Kuhn M (2008) Building predictive models in R using the caret Package. *Journal of Statistical Software* 28: 1–26.

Larondelle N, Hamstead ZA, Kremer P, et al. (2014) Applying a novel urban structure classification to compare the relationships of urban structure and surface temperature in Berlin and New York City. *Applied Geography* 53: 427–437. DOI: 10.1016/j.apgeog.2014.07.004.

Lu Y, Nakicenovic N, Visbeck M, et al. (2015) Policy: five priorities for the un sustainable development goals. *Nature* 520: 432–433. DOI: 10.1038/520432a.

McPhearson T, Hamstead ZA and Kremer P (2014) Urban ecosystem services for resilience planning and management in New York City. *Ambio* 43(4): 502–515. DOI: 10.1007/s13280-014-0509-8.

Mitz E, Kremer P, Larondelle N, et al. (2021) Structure of Urban landscape and surface temperature: a case study in Philadelphia, PA. *Frontiers in Environmental Science* 9(March): 592716. DOI: 10.3389/fenvs.2021.592716.

Mitz E, Kremer P, Larondelle N, et al. (2021) Structure of Urban landscape and surface temperature: a case study in Philadelphia, PA. *Frontiers in Environmental Science* 9(March): 35. DOI: 10.3389/fenvs.2021.592716.

Morales SE, Biswas A, Herndl GJ, et al. (2019) Global structuring of phylogenetic and functional diversity of pelagic fungi by depth and temperature. *Frontiers in Marine Science* 6: 131. DOI: 10.3389/fmars.2019.00131.

NYC Department of City Planning (2021) *MapPluto Database*. New York State Government.

Oke T. R. (1995) Classics in physical geography revisited: Sundborg, Å. 1951: Climatological studies in Uppsala with special regard to the temperature conditions in the urban area. Geographica 22. Progress in

Physical Geography. *Progress in Physical Geography: Earth and Environment* 19: 107–113. DOI: 10.1177/030913339501900105.

Oliveira S, Oehler F, San-Miguel-Ayanz J, et al. (2012) Modeling spatial patterns of fire occurrence in Mediterranean Europe using Multiple Regression and Random Forest. *Forest Ecology and Management* 275: 117–129. DOI: 10.1016/j.foreco.2012.03.003.

OS B and AA A (2016) Change detection in land surface temperature and land use land cover over Lagos Metropolis, Nigeria. *Journal of Remote Sensing & GIS* 5(3): 1–8. DOI: 10.4172/2469-4134.1000171.

Palme M, Inostroza L and Salvati A (2018) Technomass and cooling demand in South America: a superlinear relationship? *Building Research & Information* 46(8): 864–880. DOI: 10.1080/09613218.2018.1483868/SUPPL_FILE/RBRI_A_1483868_SM2255.PDF.

Sanchez L and Reames TG (2019) Cooling Detroit: a socio-spatial analysis of equity in green roofs as an urban heat island mitigation strategy. *Urban Forestry and Urban Greening* 44: 126331. DOI: 10.1016/j.ufug.2019.04.014.

Stewart ID and Oke TR (2012) Local climate zones for Urban temperature studies. *Bulletin of the American Meteorological Society* 93(12): 1879–1900. DOI: 10.1175/BAMS-D-11-00019.1.

Stewart ID, Oke TR and Krayenhoff ES (2014) Evaluation of the 'local climate zone' scheme using temperature observations and model simulations. *International Journal of Climatology* 34(4): 1062–1080. DOI: 10.1002/JOC.3746.

Stewart JD, Kremer P, Shakya KM, et al. (2021) Outdoor atmospheric microbial diversity is associated with urban landscape structure and differs from indoor-transit systems as revealed by mobile monitoring and three-dimensional spatial analysis. *Frontiers in Ecology and Evolution* 9: 9. https://www.frontiersin.org/article/10.3389/fevo.2021.620461

Streutker D (2003) Satellite-measured growth of the urban heat island of Houston, Texas. *Remote Sensing of Environment* 85(3): 282–289. DOI: 10.1016/S0034-4257(03)00007-5.

Susca T, Gaffin SR and Dell'Osso GR (2011) Positive effects of vegetation: Urban heat island and green roofs. *Environmental Pollution* 159: 2119–2126. DOI: 10.1016/j.envpol.2011.03.007.

United States Census Burough (2016) *New York City Census*. https://www.census.gov/quickfacts/newyorkcitynewyork.

Voogt JA and Oke TR (1998) Effects of urban surface geometry on remotely-sensed surface temperature. *International Journal of Remote Sensing* 19: 895–920. DOI: 10.1080/014311698215784.

Walker B, Holling CS, Carpenter SR, et al. (2004) Resilience, adaptability and transformability in social-ecological systems. *Ecology and Society* 9: 5. DOI: 10.5751/ES-00650-090205.

Weiss N (n.d.). wPerm: Permutation tests. R package version 1.0. 1.

Wong MS, Peng F, Zou B, et al. (2016) Spatially analyzing the inequity of the hong kong urban heat island by socio-demographic characteristics. *International Journal of Environmental Research and Public Health* 13: 317. DOI: 10.3390/ijerph13030317.

Yang J, Zhan Y, Xiao X, et al. (2020) Investigating the diversity of land surface temperature characteristics in different scale cities based on local climate zones. *Urban Climate* 34: 100700. DOI: 10.1016/J.UCLIM.2020.100700.

Yang X and Li Y (2015) The impact of building density and building height heterogeneity on average urban albedo and street surface temperature. *Building and Environment* 90: 146–156. DOI: 10.1016/J.BUILDENV.2015.03.037.

Zhou W, Huang G and Cadenasso ML (2011) Does spatial configuration matter? Understanding the effects of land cover pattern on land surface temperature in urban landscapes. *Landscape and Urban Planning* 102(1): 54–63. DOI: 10.1016/j.landurbplan.2011.03.009.

Zhou W, Pickett STA and Cadenasso ML (2017) Shifting concepts of urban spatial heterogeneity and their implications for sustainability. *Landscape Ecology* 32(1): 15–30. DOI: 10.1007/s10980-016-0432-4.